Pure Appl. Chem., Vol. 71, No. 11, pp. 2107–2115, 1999.
Printed in Great Britain.

Ultrafast excitation transfer and relaxation in linear and crossed-linear arrays of porphyrins*

Seiji Akimoto[1], Tomoko Yamazaki[1], Iwao Yamazaki[1,†], Aiko Nakano[2] and Atsuhiro Osuka[2]

[1]*Graduate School of Engineering, Department of Molecular Chemistry, Hokkaido University, Sapporo 060-8628, Japan*
[2]*Graduate School of Chemistry, Department of Chemistry, Kyoto University, Kyoto 606-8502, Japan*

Abstract: Ultrafast intramolecular excitation transfer has been studied with linear and crossed-linear porphyrin arrays by means of femtosecond time-resolved fluorescence spectroscopy. Excitation transfer from peripheral donor to a center part of acceptor occurs directly from the S_2 state of initially photoexcited donor to the acceptor S_2 state in time scales of 120–150 fs, competing with the internal conversion $S_2 \rightarrow S_1$ (150 fs). The ordinary S_1–S_1 energy transfer is much longer time scale of 100 ps. The rate constants of S_2–S_2 and S_1–S_1 energy transfers were in acceptable agreement with the theoretical estimation.

INTRODUCTION

Photochemical processes such as electron transfer and excitation transfer are expected to occur very fast in highly organized molecular systems in which reacting molecules are located with close proximity and optimal orientation. Molecules in such systems can be coupled to an adjacent molecule with relatively strong intermolecular interaction, and therefore they may undergo ultrafast photochemical reaction with its time scales ranging in the order of ten femtosecond to several hundred femtosecond. Then the reaction might compete with or exceeds over the intramolecular energy relaxations such as internal conversion (IC), vibrational relaxation (VR) and internal vibrational redistribution (IVR) in each constituent molecule. It has long been recognized that these intramolecular relaxation processes are extremely fast in condensed matters like solution and solid states [1]. Very few information is available concerning the time scale of these processes. However recent progress of femtosecond time-resolved spectroscopies has revealed that the time scales of IC, IVR and VR are in the order of 0.1 ps and 10 ps at most.

On the other hand, recent studies on photophysical processes in organized molecular systems have demonstrated that the photoinduced electron transfer and excitation transfer occur in the time scales comparable to the intramolecular relaxation processes [2–5]. When the molecule is photoexcited into a higher excited state like S_2, then the reaction becomes involving a direct process from S_2 state before IC and VR in S_1 vibrational manifold. Furthermore, it might be possible that the reaction rate is exceeding over the energy dissipation with environments, and that the reaction proceeds with the quantum coherency being conserved during the reaction. We met these situation in several examples of photosynthetic reaction centers and some artificial macromolecules.

In the present paper, ultrafast intramolecular excitation energy transfer is discussed with linear and crossed-linear arrays of porphyrins as shown in Fig. 1. In this type of molecular systems, the energy levels of the center part of the system are slightly lower than those of peripheral porphyrin by addition of

*Lecture presented at the 4th International Symposium on Functional Dyes—Science and Technology of Functional π-Electron Systems, Osaka, Japan, 31 May–4 June 1999, pp. 2009–2160.
†*Corresponding author*: E-mail: yamia@eng.hokudai.ac.jp

arylethynyl groups at the center porphyrin. Then the excitation absorbed at the peripheral porphyrin transfers toward the center part of the system. We are concerned with nonequilibrium excitation transfer which occurs between the S_2 states of donor and acceptor before IC and thermal equilibration through VR.

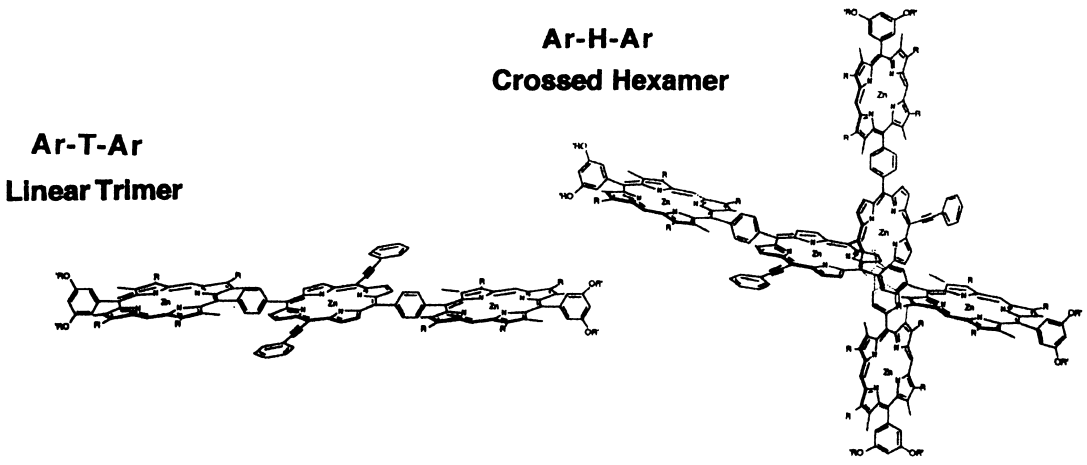

Fig. 1 Molecular arrangements of zinc porphyrins; a linear array Ar-T-Ar (left) and a crossed-linear array Ar-H-Ar (right).

EXPERIMENTAL

The two types of porphyrin arrays, a linear array (hereafter referred to as Ar-T-Ar) and a crossed-linear array (Ar-H-Ar), were synthesized by the methods described in previous papers [6,7]. Fluorescence decay curves were measured with a femtosecond fluorescence up-conversion system described in detail elsewhere [8]. The peripheral porphyrin (donor) was excited with the second harmonic of a Ti:Sapphire laser (Spectra-Physics, Tsunami, 840 nm, 80 MHz) pumped with a diode-pumped solid-state laser (Spectra-Physics, Millennia X). To avoid polarization effects, the angle between the polarizations of the excitation and probe beams were set to the magic angle by a 1/2λ plate. The instrumental response function exhibited a 200 fs (FWHM) pulsewidth. In order to reconstruct the transient spectra, the fluorescence intensities in a wavelength region of 520–620 nm were corrected using the correction factors that were obtained for matching the integrated fluorescence up-conversion signals of β-carotene with its steady-state fluorescence. All measurements were carried out at room temperature.

RESULTS

Absorption and fluorescence spectra

The absorption and fluorescence spectra of Ar-T-Ar and Ar-H-Ar in benzene solutions are shown in Figs 2 and 3 along with those of constituent moieties as donor and acceptor.

Donor monomer

Absorption spectrum consists of B-band (Soret band) in near-UV ($\lambda_{max} = 412.0$ nm) and Q band in a visible region ($\lambda_{max} = 538.5$ and 572.9 nm). Two peaks in the Q band are assigned to Q(1,0) and Q(0,0), respectively. The fluorescence spectrum of donor monomer displays intense fluorescence originating from the first excited singlet state, S_1 (Q state). This S_1 fluorescence has two peaks at 578.8 nm (Q(0,0)) and 633.0 nm (Q(0,1)). In addition to the S_1 fluorescence, a weak S_2 fluorescence is also observed that is ≈400 times less intense than the ordinary S_1 fluorescence, suggesting a significantly short lifetime.

Ar-T-Ar

The absorption band of the center part of the system (acceptor) is located at much longer wavelength than those of the donor monomer (Fig. 2). It can be seen that the absorption spectrum of the whole system is

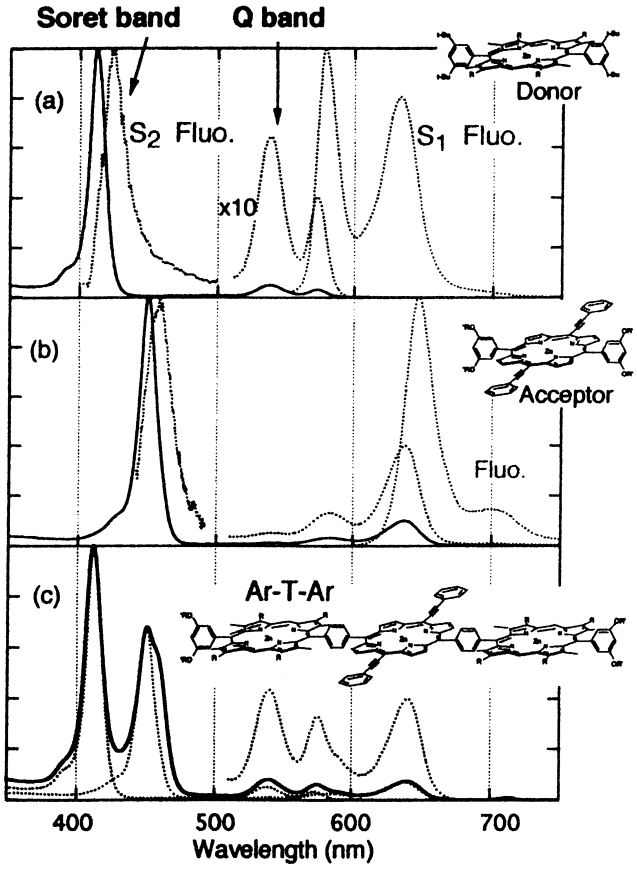

Fig. 2 Absorption and fluorescence spectra of Ar-T-Ar. (a) Donor monomer, (b) acceptor (center part) and (c) entire molecular system.

simply a sum of those of donor and acceptor parts, indicating that the interchromophore interaction is not so large ($\approx 100\,cm^{-1}$). One can find a large spectral overlap between the donor S_1 fluorescence and the acceptor absorption (Q band). Similarly, another large spectral overlap can be seen between the donor S_2 fluorescence and the acceptor S_2 absorption (B band), which means a possibility of a direct excitation transfer between the S_2 states of donor and acceptor.

Ar-H-Ar

Similar spectra were obtained for the crossed linear hexamer array (Fig. 3). The absorption spectrum of the center part of acceptor is similar to the case of Ar-T-Ar for Q band, while for B band it splits into two bands due to the exciton interaction of porphyrin dimer. The absorption intensity at the B band is significantly large associated with increasing number of peripheral porphyrin rings.

In these two cases, Ar-T-Ar and Ar-H-Ar, one can photoexcite the B band of donor selectively at 420 nm, and examine the excitation transfer kinetics by monitoring the S_2 and S_1 fluorescence of the donor and acceptor. It is expected that the femtosecond time-resolved fluorescence spectrum exhibits the donor fluorescence in earlier time, particularly at very short time the donor S_2 fluorescence, and then goes to the acceptor S_1 fluorescence.

Fluorescence decay kinetics of the donor monomer

When the donor monomer is excited at 420 nm (B band), it emits two fluorescence emissions from S_2 and S_1 around 430 and 600 nm, respectively. The intensity ratio of the two emissions are 1:400. The fluorescence signal of the B band (470 nm) is represented by a monoexponential decay with a time constant of 150 ± 10 fs. In contrast to the S_2 fluorescence, the fluorescence monitored at 580 nm (Q(0,0)

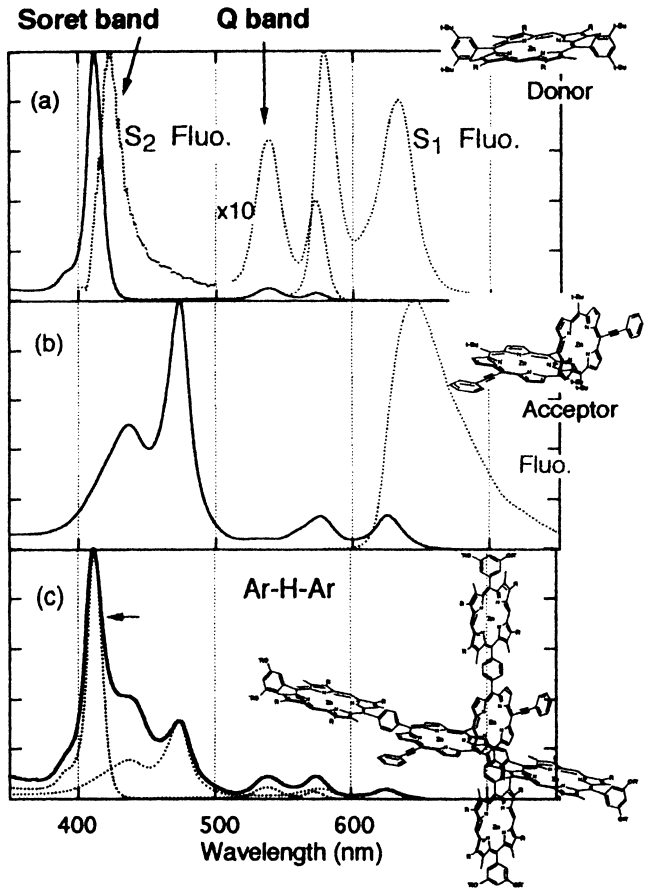

Fig. 3 Absorption and fluorescence spectra of Ar-H-Ar. (a) Donor monomer, (b) Acceptor (center part) and (c) entire molecular system.

band) is best represented by a sum of a rise of 150 ± 10 fs and a decay of 1.5 ns. The fast rise component shows a good correlation between the B state population decay and the Q state population rise. The time constant of 150 fs can be associated with the $S_2 \rightarrow S_1$ internal conversion. This time constant is in rough agreement with the intensity ratio of S_2 and S_1 fluorescences.

Time-resolved fluorescence spectra

Fluorescence lifetimes are summarized in Table 1. In Ar-T-Ar, the donor S_2 emission exhibits a short decay with the decay constant of 74 fs, and the acceptor S_2 emission includes a rise component and also a very short decay at 470 nm. Note that the S_2 fluorescence of donor monomer decays with the time constant of 150 fs which corresponds to the internal conversion. It follows that the S_2 fluorescence decay time of donor in Ar-T-Ar is reduced to a half in the absence of the acceptor. This means that the IC process ($S_2 \rightarrow S_1$) competes with a direct energy transfer between the S_2 states of donor and acceptor. In Ar-H-Ar, similar decay kinetics are obtained.

The S_1 fluorescence decay profiles in both two cases depend on monitoring wavelength, and includes fast and slowly decaying components. The short decay components indicate vibrational relaxation in the S_1 vibrational manifold.

Figs 4 and 5 show the time-resolved fluorescence spectra of Ar-T-Ar and Ar-H-Ar, respectively. In the two cases, the spectra changes within 2 ps. Four kinds of emission bands are involved in the spectra: the donor $S_2 \rightarrow S_0$ fluorescence (shorter than 500 nm) mixed with the acceptor S_2 fluorescence, the donor $S_2^* \rightarrow S_0^*$ hot fluorescence (500–570 nm), the donor S_1 fluorescence (580–630 nm) and the acceptor S_1 fluorescence (630–700 nm). The donor S_2 fluorescence disappears within 200 fs and then the donor S_1

Table 1 Fluorescence decay curve analyses: the lifetimes and amplitudes of components of exponential decays

	Monitoring wavelengths			
	S_2 fluorescence		S_1 fluorescence	
Compounds	430 nm	470 nm	590 nm	650 nm
Donor monomer	150 fs		1.5 ns	
Ar-M-Ar		81 fs (−0.95)	113 fs (0.42)	570 fs (−0.87)
(Center part)		455 fs (1.0)	1.8 ps (0.22)	
			1.0 ns (0.06)	1.5 ns (1.0)
Ar-T-Ar	74 fs	70 fs (−0.61)	102 fs (−0.61)	102 fs (−0.99)
		130 fs (1.0)	1.2 ps (0.59)	2.0 ps (0.49)
			4.6 ps (0.41)	1.5 ns (0.51)
Ar-D-Ar		67 fs	278 fs (0.63)	250 fs (−0.47)
(Center part)			1.9 ps (0.28)	
			1.5 ns (0.09)	1.5 ns (1.0)
Ar-H-Ar	28 fs (−0.47)	49 fs (−0.99)	82 fs (−0.91)	94 fs (−0.76)
	68 fs (1.0)	54 fs (1.0)	1.3 ps (0.55)	2.4 ps (0.46)
			6.0 ps (0.45)	22 ps (0.54)

and acceptor S_1 fluorescence rise in the same time region. One should note that the acceptor $S_1^* \rightarrow S_0^*$ hot fluorescence appears also in this time region. Combining these spectral changes with the decay constants mentioned above, we analyzed quantitatively the kinetics of the excitation transfer and the relaxation processes on the basis of a reaction scheme given in the next section.

DISCUSSION

Fluorescence decay analyses

In order to derive rate constants of the reaction processes involved in the photoexcited molecular assemblies of Ar-T-Ar and Ar-H-Ar, the fluorescence decay curves were analyzed on the basis of a reaction scheme shown in Fig. 6. The rate equations for the energy transfer and the relaxation processes can be expressed in the following forms:

$$\frac{d[D_2]}{dt} = -\lambda_1[D_2], \qquad \lambda_1 = k_{F2}^D + k_{Q2}^D + k_2 \tag{1}$$

$$\frac{d[A_2]}{dt} = k_2[D_2] - \lambda_2[A_2], \qquad \lambda_2 = k_{21} + k_{F2}^A + k_{Q2}^A \tag{2}$$

$$\frac{d[D_1]}{dt} = k_{Q2}^D[D_2] + k_{21}[A_2] - \lambda_3[D_1], \qquad \lambda_3 = k_{F1}^D + k_{Q1}^D + k_1 \tag{3}$$

$$\frac{d[A_1]}{dt} = k_{Q2}^A[A_2] + k_1[D_1] - \lambda_4[A_1], \qquad \lambda_4 = k_{F1}^A + k_{Q1}^A \approx k_{Q1}^A \tag{4}$$

where $[D_1]$ and $[D_2]$ ($[A_1]$ and $[A_2]$) are the concentrations of excited donor (acceptor) molecules in S_1 and S_2, respectively, and k's are the rate constants for the processes shown in Fig. 6. The general solutions of the differential equations Eqns 1–4 can be obtained as follows:

$$[D_2] = a_1 e^{-\lambda_1 t}, \qquad [A_2] = b_1 e^{-\lambda_1 t} + b_2 e^{-\lambda_2 t} \tag{5 and 6}$$

$$[D_1] = c_1 e^{-\lambda_1 t} + c_2 e^{-\lambda_2 t} + c_3 e^{-\lambda_3 t}, \qquad [A_1] = d_1 e^{-\lambda_1 t} + d_2 e^{-\lambda_2 t} + d_3 e^{-\lambda_3 t} + d_4 e^{-\lambda_4 t} \tag{7 and 8}$$

Taking the initial conditions, $[D_2] = a_1$, $[A_2] = [D_1] = [D_2] = 0$ at $t = 0$, we obtain the solutions with

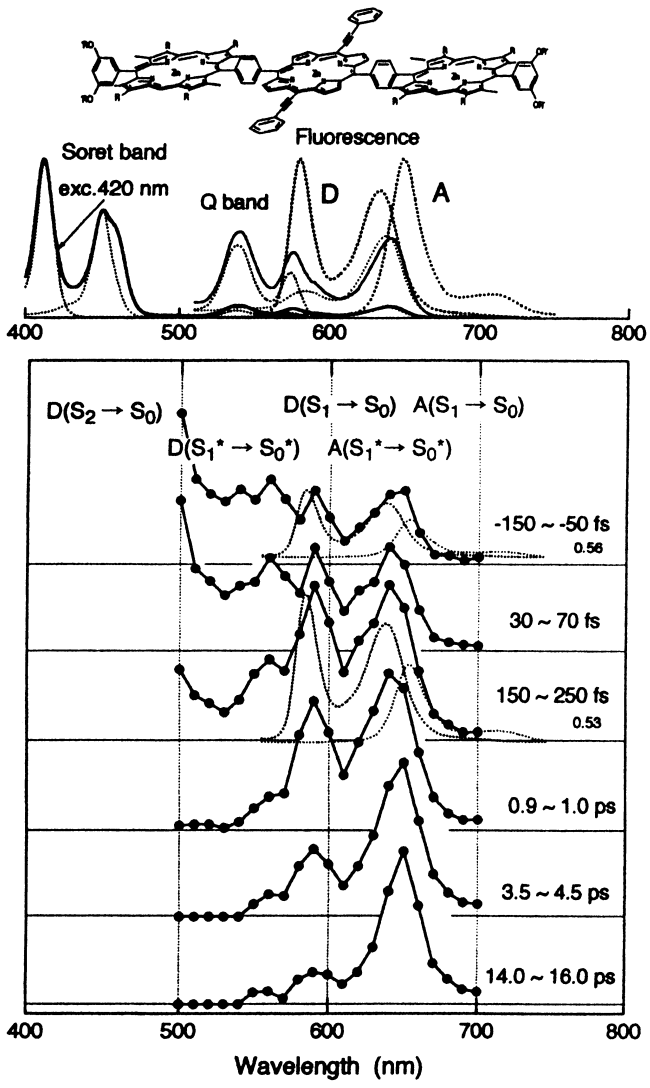

Fig. 4 Time-resolved fluorescence spectra of Ar-T-Ar. The excitation wavelength is 420 nm. Absorption and steady-state fluorescence spectra are shown in the top.

the coefficients:

$$b_1 = -k_2 a_1 (\lambda_A - \lambda_B)^{-1}, \qquad b_2 = k_2 a_1 (\lambda_A - \lambda_B)^{-1} \tag{9 and 10}$$

$$c_1 = \frac{a_1(\lambda_2 - \lambda_3)}{(\lambda_1 - \lambda_2)(\lambda_1 - \lambda_3)} \{k_2 k_{21} - (\lambda_1 - \lambda_2)(k_{F2}^D + k_{Q2}^D)\} \tag{11}$$

$$c_2 = -\frac{a_1(\lambda_1 - \lambda_3)}{(\lambda_1 - \lambda_2)(\lambda_2 - \lambda_3)} k_2 k_{21} \tag{12}$$

$$c_3 = -\frac{a_1(\lambda_1 - \lambda_2)}{(\lambda_2 - \lambda_3)(\lambda_1 - \lambda_3)} \{k_2 k_{21} + (\lambda_2 - \lambda_3)(k_{F2}^D + k_{Q2}^D)\} \tag{13}$$

Substituting the fluorescence lifetimes into Eqns 5–13, one can obtain the rate constants. The fluorescence lifetimes used here are listed in Tables 1 and 2.

The results of numerical analyses are summarized in the right half of Table 2 for k_1, k_2 and k_{21}. A striking feature is that the excitation transfer between the S_2 states of donor and acceptor is much faster than those between the S_1 states by a factor of 30 in Ar-T-Ar and by a factor of 8 in Ar-H-Ar; the

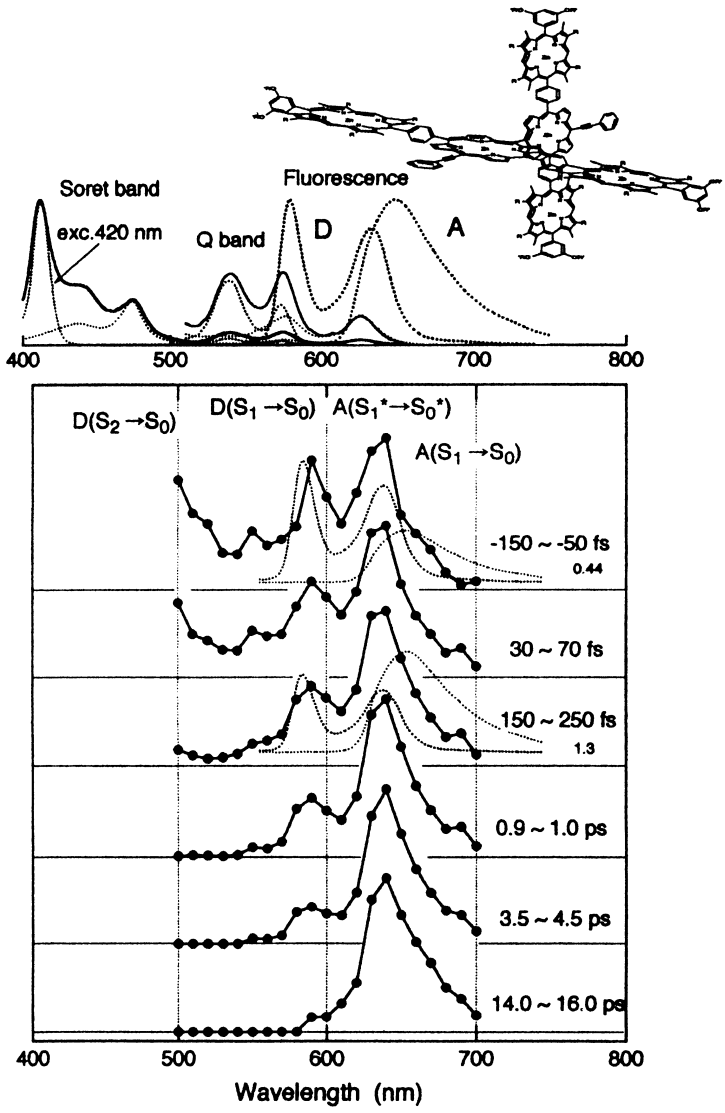

Fig. 5 Time-resolved fluorescence spectra of Ar-H-Ar. The excitation wavelength is 420 nm. Absorption and steady-state fluorescence spectra are shown in the top.

time scales are 145 fs and 124 fs, respectively. The rest of the relaxation process from S_2 state proceeds through the internal conversion $S_2 \rightarrow S_1^*$, followed by the vibrational relaxation in the S_1 vibrational manifold in 600 fs from the vibrationally hot S_1^* state. Then the ordinary S_1–S_1 excitation transfer occurs in longer time scales, 6 ps in Ar-T-Ar and 4.6 ps in Ar-H-Ar.

The experimental finding that the excitation transfer occurs directly from the S_2 state is supported from the theoretical estimation of the transfer rates. According to the usual Förster mechanism, the rate constant for the dipole-dipole energy transfer is given by the following equation:

$$k_{DA} = \frac{9000\kappa^2 \ln 10}{128\pi^5 n^4 N \tau_0 R^6} \int \frac{f_D(\nu)\varepsilon_A(\nu)}{\nu^4} d\nu, \qquad \kappa = \cos\phi_{DA} - 3\cos\phi_D \cos\phi_A \tag{14}$$

where ν is wavenumber, $\epsilon(\nu)$ is molar extinction coefficient, $f(\nu)$ is the normalized spectral distribution of donor fluorescence, N is Avogadro's number, τ_0 is the natural fluorescence lifetime of donor, n is refractive index of solvent, and R is the distance between donor and acceptor. In the orientation factor κ, ϕ_{DA} is the angle between the transition moments of donor and acceptor, ϕ_D and ϕ_A are the angles between the respective transition moments and the distant vector **R**. We calculated the transition moments and

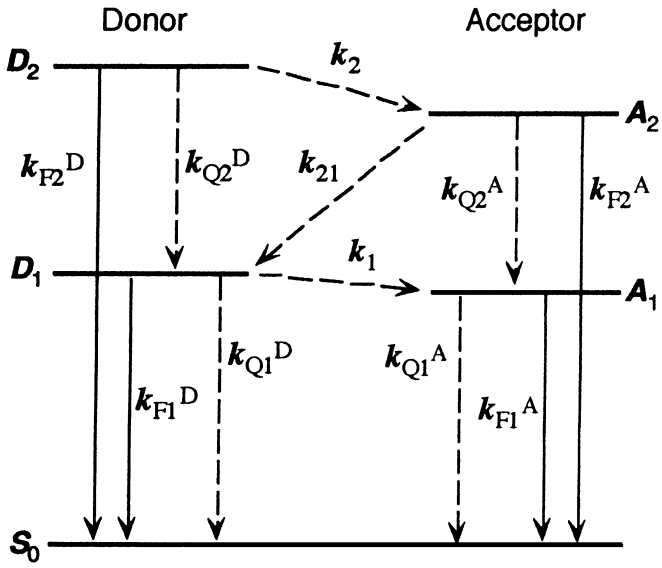

Fig. 6 Energy levels of donor and acceptor parts, the processes of excitation transfer and energy relaxation, and the symbols of their rate constants. Solid lines are radiative processes and broken lines are nonradiative processes. D_2 (D_1) and A_2 (A_1) denote the S_2 (S_1) states of donor and acceptor, respectively.

Table 2 Fluorescence decay curve analyses: The lifetimes and amplitudes of components of exponential decays

	Fluorescence lifetimes (ps)				Rate constants ($10^{12}\,s^{-1}$)		
Molecules	$(\lambda_1)^{-1}$	$(\lambda_2)^{-1}$	$(\lambda_3)^{-1}$	$(\lambda_4)^{-1}$	k_2	k_{21}	k_1
Ar-T-Ar	0.074	0.130	4600	1.5×10^6	6.85	1.0	0.22
Ar-H-Ar	0.068	0.054	6000	22	8.04	0.17	1.06

the natural lifetimes for the B band and the Q band. The calculated k_{DA}'s are $8.4\times10^{12}\,s^{-1}$ for the S_2–S_2 transfer and $0.8\times10^{12}\,s^{-1}$ for the S_1–S_1 transfer in Ar-T-Ar, and $3.4\times10^{12}\,s^{-1}$ for the S_2–S_2 transfer and $0.7\times10^{12}\,s^{-1}$ for the S_1–S_1 transfer in Ar-H-Ar. It is found that the relative magnitude of the rates between the S_2–S_2 and S_1–S_1 transfers is in acceptable agreement with the experimental results listed in Table 2.

It is worth noting that the time scales of the S_2–S_2 excitation transfers might be comparable to those of IVR with reference to the previous studies shown in [2–4]. In our previous paper [9], we reported excitation delocalization in circular arrangements of zinc porphyrins, which occurs in 80–500 fs in the higher excitonic states. The present study provides another example of photophysical process among higher excited states.

ACKNOWLEDGEMENT

This work was supported by Ministry of Education, Science, and Culture of Japan, A Grant-in-Aid for Scientific Research on Priority Areas No. 729 (11223203), and Scientific Research (Category A) No. 9304056.

REFERENCES

1 R. M. Hochstrasser, R. B. Weisman. In *Radiationless Transitions* (S. H. Lin, ed.), p. 317. Academic Press, New York (1980).

2 A. Mokhtari, J. Chesnoy, A. Laubereau. *Chem. Phys. Lett.* **155**, 593 (1989).

3 I. Martini, G. V. Hartland. *J. Phys. Chem.* **100**, 19764 (1996).

4 Y. Jiang, G. J. Blanchard. *J. Phys. Chem.* **99**, 7904 (1995).

5 M. Wall, S. Akimoto, T. Yamazaki, N. Ohta, I. Yamazaki, T. Sakuma, H. Kido. *Bull. Chem. Soc. Jpn* **72**, 1475 (1999).

6 A. Nakano, A. Osuka, I. Yamazaki, T. Yamazaki, Y. Nishimura. *Angew. Chem. Int. Ed.* **37**, 3023 (1998).

7 A. Nakano, T. Yamazaki, A. Osuka, Y. Nishimura, S. Akimoto, I. Yamazaki, A. Osuka. Unpublished results.

8 S. Akimoto, S. Takaichi, T. Ogata, Y. Nishimura, I. Yamazaki, M. Mimuro. *Chem. Phys. Lett.* **260**, 147 (1996).

9 I. Yamazaki, S. Akimoto, T. Yamazaki, H. Shiratori, A. Osuka. *Acta Phys. Polonica A* **95**, 105 (1999).